A Quadratic Basis Function, Quadratic Geometry, High Order Panel Method.

David J. Willis* Jaime Peraire †

Jacob K. White‡

Massachusetts Institute Of Technology, 77 Massachusetts Ave., Cambridge, MA 02139, USA.

Most panel method implementations use both low order basis function representations of the solution and flat panel representations of the body surface. Although several implementations of higher order panel methods exist, difficulties in robustly computing the self term integrals remain. In this paper, methods for integrating the single and double layer self term integrals are presented. The approaches are conceptually simple and robust. The paper considers quadratic basis functions to represent the solution, while the geometry of the body is approximated using piecewise parametric quadratic patches. Increased convergence rates are demonstrated for cases where the quadratic basis functions on quadratic curved panels are used. The quadratic panel method converges at a rate proportional to the cube of the panel side length (or $NP^{-\frac{3}{2}}$, where NP is the number of panels).

Nomenclature

$\|J\|$	Determinant of the Mapping Jacobian
x	Point position
S	Area
ϕ	Perturbation Potential
Ψ	Result of the single layer integration
Φ	Result of the double layer integration
σ	Source or Single Layer Strength
μ	Doublet or Double Layer Strength
s, t	Surface Parameters
V	Vandermonde Matrix
$\vec{C}$	Vector of Polynomial Coefficients
ξ, η	Panel Coordinate System
P, Q	Polynomial Approximations
$n, \hat{n}$	Normal direction
Subscript	
f	Flat Panel
c	Curved Panel
i	Variable number
m, n	Index Number

*Graduate Student, Department of Aeronautics and Astronautics, 77 Massachusetts Ave., Cambridge, MA 02139.

†Professor, Department of Aeronautics and Astronautics, 77 Massachusetts Ave., Cambridge, MA 02139.

‡Professor, Department of Electrical Engineering and Computer Science, 77 Massachusetts Ave., Cambridge, MA 02139.

x x-Direction
y y-Direction
Z z-Direction

I. Introduction

Many Boundary Element Method (BEM) implementations use low order basis functions (constant and linear variations) to represent the solution on a flat panel discretization of the surface.[1–3] The drawback of using flat panel representations of a curved surface is that regardless of how well the solution is approximated using higher order basis functions, the maximum possible convergence rate will always be limited by the rate of convergence of the discrete geometry to the actual geometry. In order to achieve highly accurate numerical solutions over curved surfaces, a large number of flat panels will be required. Using fast algorithms such as the Fast Multipole Method[5] and the precorrected-FFT,[4] users are able to converge to their desired accuracy through dramatically increasing the number of panels.

Since the solution of boundary element methods using pFFT and Fast Multipole Methods scale nearly linearly with the number of panels, there is little room for dramatic improvement of the solution time vs. accuracy for low order panel methods. In order to attain a more accurate solution in a more timely fashion, one must consider increasing the order of the numerical approximation of the governing BIE. Several implementations of high order boundary element methods exist in both two dimensions and three dimensions.[10–16,18–20]

One of the main difficulties in developing high order solutions to the potential flow problem is the lack of available techniques to accurately evaluate the required high order curved panel integrals. Although methods for the evaluation of the integral expressions[6,10,14] have been presented, difficulties remain when evaluating the self term integrals. Significant care is required when evaluating these integrals due to the singularity of the integral equation kernel at these points. Traditional quadrature schemes and panel splitting approaches perform poorly for self term integrals as well as near self term integration. One common approach is the use of adaptive quadrature approaches.[10]

In this paper, we present techniques for evaluating the curved panel single and double layer potential self term. Using the integration approaches developed, it is shown that the high order panel method solver has increased solution convergence rates compared with traditional flat panel approaches.

II. Potential Flow Boundary Integral Equation

Although several formulations exist for the solution of the potential flow around bodies, in this paper we are concerned with the potential solution to the Green's Theorem formulation:

$$\phi(x) = -\frac{1}{4\pi}\int_S \phi \frac{\partial}{\partial n}\left(\frac{1}{\|x-x'\|}\right) dS' + \frac{1}{4\pi}\int_S \left(\frac{\partial \phi}{\partial n}\right)\frac{1}{\|x-x'\|} dS'. \tag{1}$$

The equation is solved by specifying the single layer strength (traditionally labeled the source distribution or $\sigma(x) = \frac{\partial \phi}{\partial n}$) to enforce the no penetrating flux boundary condition. The remaining unknown is the double layer potential ϕ on the surface of the body. In traditional panel methods, the ϕ is the perturbation potential otherwise known as the doublet strength, typically represented as $\mu(x) = \phi$. When lifting surfaces are considered, one must also include a wake discretization to represent the vorticity carrying wake in the domain and specify the wake strength using a Kutta condition.[8] In this paper, we focus on the solution of non-lifting potential flow problems.

III. Parametrized Quadratic Panel Patches With Quadratic Basis Functions

In order to construct the BEM solution, discrete approximations to both the surface of the body and the solution must be made. The geometry in the current panel method implementation is described using parametrized triangular quadratic patches.[21] Each of the patches consists of a surface described by the following parametric representation:

$$X(s,t) = a_x s^2 + b_x t^2 + c_x s \cdot t + d_x s + e_x t + f_x \tag{2}$$

$$Y(s,t) = a_y s^2 + b_y t^2 + c_y s \cdot t + d_y s + e_y t + f_y \tag{3}$$

$$Z(s,t) = a_z s^2 + b_z t^2 + c_z s \cdot t + d_z s + e_z t + f_z \tag{4}$$

The coefficients a_i through f_i are determined from the nodes defining the curved panel patch. The representation of the parametrization is shown in figure 1.

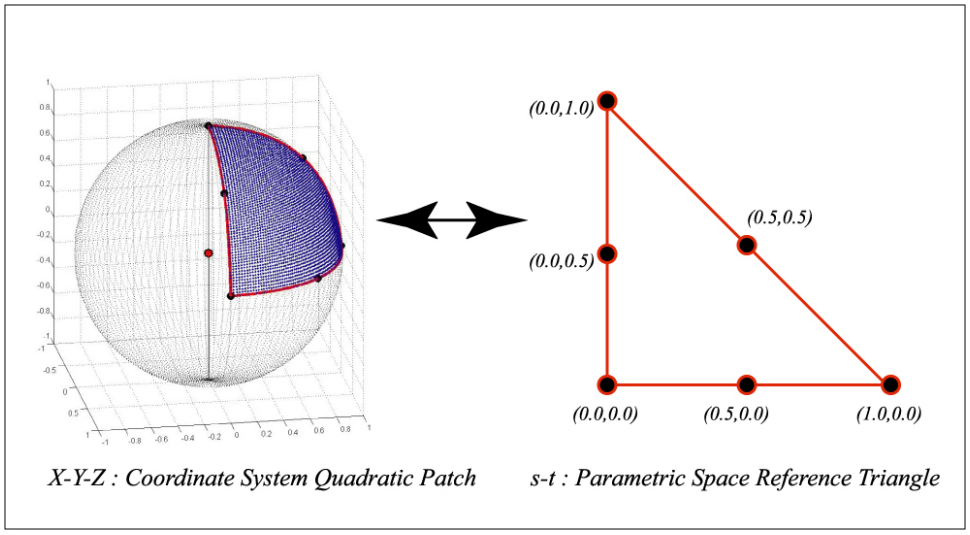

Figure 1. The relationship between the quadratically curved panel and the flat parametric triangle. The curved panel in this example is a $\frac{1}{8}$ segment of a sphere.

Parametric quadratic basis functions are used such that the patch geometry definition is consistent with the basis function definition.[21] These basis functions for a given panel are presented pictorially in figure 2.

IV. Panel Integration Approaches for Non-Self Term Integrals

High order methods currently consider adaptive quadrature schemes,[10] expansions[14] and semi-analytical approaches[6,16] for the evaluation of curved panel integrals. In the panel method implementation presented in this paper, the nearby non-self term panel integrals are computed using the method developed by Wang et al.,[6] the far field interactions are computed using a quadrature approximation, while the self term panel integrals are evaluated using the methods described in section V. Although the Wang et al. method is used for nearby panels, it should be noted that the methods presented for the self term integrals can be extended to compute the non-self term integrals, however, they are typically less efficient than the Wang et al. approach. The Wang et al. method does not work well for the self term evaluation in this quadratic panel method setting due to:

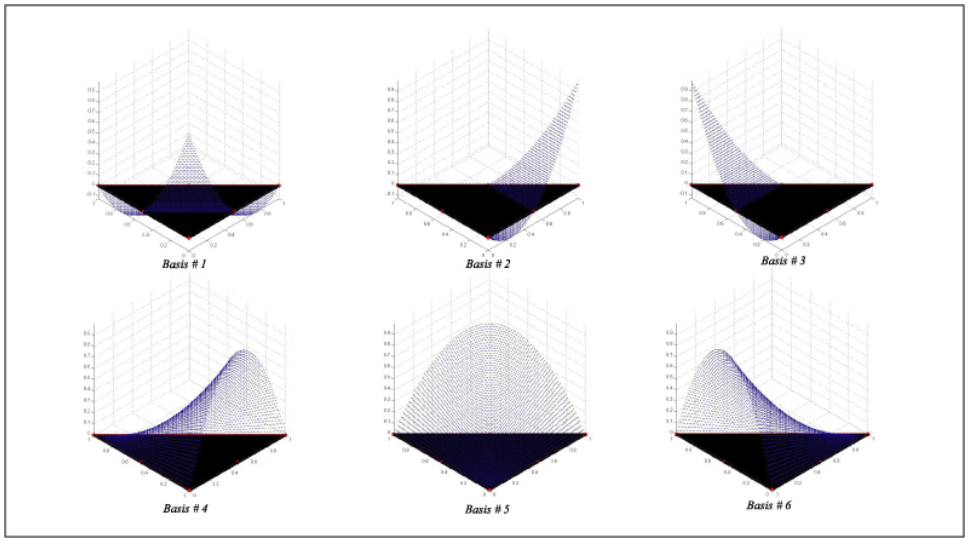

Figure 2. The 6-quadratic basis functions on the reference triangle.

1. The method does not work for the self-term double layer integral evaluation. This is due to the inability to form a ratio between the kernel for a flat panel and the kernel for a curved panel. This is shown below in the equivalent flat panel representation of the curved panel integral:

$$\Phi(x) = \int_{S'_f} \mu(x') \frac{\partial}{\partial n} \left(\frac{1}{\|x - x'_f\|} \right) \left(\frac{\frac{\partial}{\partial n} \left(\frac{1}{\|x - x'_f\|} \right)}{\frac{\partial}{\partial n} \left(\frac{1}{\|x - x'_c\|} \right)} |J| \right) dS'_f, \tag{5}$$

   but:

$$K_{\frac{\partial}{\partial n}\left(\frac{1}{r}\right)} = \frac{\frac{\partial}{\partial n} \left(\frac{1}{\|x - x'_f\|} \right)}{\frac{\partial}{\partial n} \left(\frac{1}{\|x - x'_c\|} \right)} \tag{6}$$

   Is undefined at $x = x'$ and zero elsewhere. Hence, it is not possible to fit a polynomial accurately through this representation.

2. For the self term curved panel integration of the single layer potential, the method works well for surfaces with a single radius of curvature where the evaluation point lies. In general, when surfaces of non-constant curvature are considered, it is challenging to determine a mapping in which the self term curved-to-flat panel transformation is easily fitted with a polynomial. Although the Wang et al. method can be applied, the accuracy of the approach will typically be reduced due to the difficulties of accurately fitting a polynomial to represent the mapping from a curved to a flat panel.

V. Panel Integration: The Self Term Integrals

We have developed methods for computing both the double layer potential self term integrals and present them in the following sections. In addition, we present a single layer integration approach which corresponds closely to currently available methods,[10] but differs in certain finer details of the implementation. It should be noted that the methods developed in this section can be extended to computing non-self term integrals, however, would likely be more costly than the Wang et al. approach.

A. Single Layer Integrals: The Self Term Integral

Although the self term integration for the single layer which is used is similar to the Wang et al. approach and those traditionally used,[10] the differences introduced in this computation, albeit small, are important to improve the accuracy of the quadratically curved panel integrals.

1. Background Theory

The single layer potential self term integration is performed numerically after appropriately transforming the curved panel into a flat panel (with curved edges). Following the transformation, the panel integral is evaluated using quadrature in cylindrical coordinates. The transformation to cylindrical coordinates to desingularize the integrand was presented by Hess and Smith[17] in their analytical computation approaches for flat panel integrals, and the ideas have been further used in numerical implementations for higher order.[10] The background theory of the method used in this paper is described below:

1. Consider the integral governing the self term single layer on a curved panel:

$$\Psi(x) = \int_{S'_c} \sigma(\xi'_c, \eta'_c) \frac{1}{\|x - x'_c\|} dS'_c, \tag{7}$$

where $\sigma(\xi', \eta')$ is the basis function representation of the single layer strength on the panel.

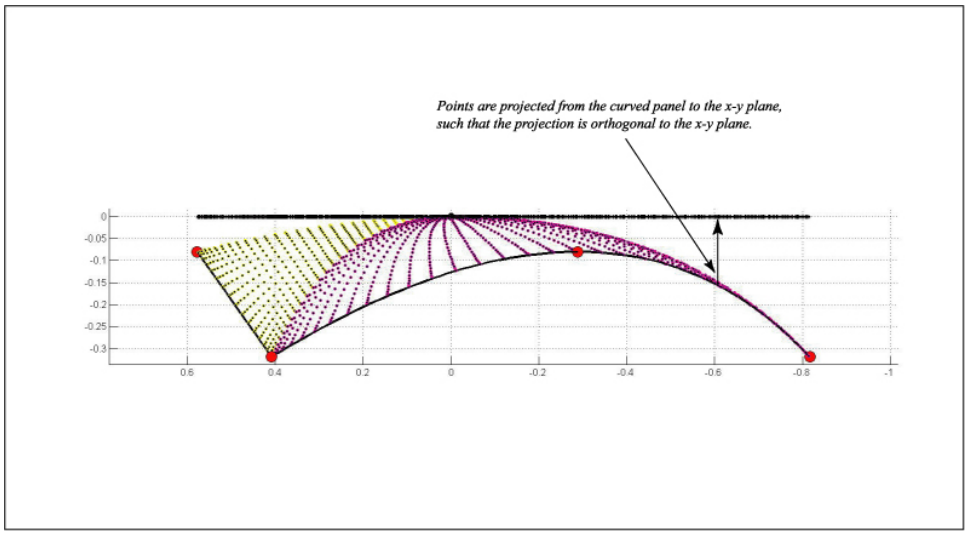

Figure 3. The orthonormal projection shown for a large selection of points on the curved panel to the tangent plane. Notice that the curved panel is projected onto the tangent plane in a manner that is normal to the tangent plane.

2. Project the curved panel geometry using an orthonormal projection onto the tangent plane at the evaluation point as shown in figure 3. As a result the integral over the flat tangent plane is:

$$\Psi(x) = \int_{S'_f} \sigma(\xi'_c, \eta'_c) \frac{1}{\|x - x'_c\|} |J| dS'_f, \tag{8}$$

where $|J|$ is the determinant of the Jacobian due to the orthonormal mapping. The value of $|J|$ evaluated across the flat panel will be smooth assuming large distortions are not encountered in the mapping.

3. As in the Wang et al. method,[6] multiply and divide the integrand by $\frac{1}{\|x-x'_f\|}$:

$$\Psi(x) = \int_{S'_f} \sigma(\xi'_c, \eta'_c) \frac{1}{\|x - x'_f\|} \left(\frac{\|x - x'_f\|}{\|x - x'_c\|} |J| \right) dS'_f. \tag{9}$$

4. Combine the basis representation polynomial ($\sigma(\xi'_c, \eta'_c)$) with the polynomial representation of the mapping, into a single polynomial representation $Q(x'_c)$, and the integral becomes:

$$\Psi(x) = \int_{S'_f} Q(x'_c) \frac{1}{\|x - x'_f\|} dS'_f \tag{10}$$

5. Equation 10 is then re-written in polar coordinates as:

$$\Psi(x) = \int_{\theta=0}^{\theta=2\pi} \int_{r=0}^{r=R(\theta)} Q(r'_f, \theta'_f) \frac{1}{\|r'_f\|} r' d\theta' dr' \tag{11}$$

6. Which, when simplified becomes:

$$\Psi(x) = \int_{\theta=0}^{\theta=2\pi} \int_{r=0}^{r=R(\theta)} Q(r'_f, \theta'_f) d\theta' dr' \tag{12}$$

7. The resulting integral is simple to evaluate first analytically integrating the polynomial $Q(r'_f, \theta'_f)$ in r, and then using one dimensional quadrature, for the remaining θ-integral. In cases where curved panels are significantly distorted or stretched, care should be taken as the polynomial fit will likely require significantly higher order polynomial representations for an accurate solution than when the panels are regularly shaped.

2. Implementation Approach

In order to implement the above steps in a practical manner, the following steps are used:

1. Transform the curved panel such that the tangent plane at the evaluation point lies in the $x_T - y_T$ plane, and the panel normal at the evaluation point is in the $+z_T$ direction, as shown in figure 4.

2. Determine a series of points on the curved panel which will be used to fit polynomial approximations to distribution on the panel. One can use any appropriate set of quadrature points; however, the polynomial fit will occur in $R - \Theta$ coordinates, and as such, an appropriate quadrature scheme might be similar to that used over 4-sided regions(with the sides of the rectangle being the R and Θ limits). In order to achieve a more accurate approximation to the integral, subdivision of the original panel into three panels should be performed, where the subdivision occurs by connecting lines between the vertices and the evaluation point. Figure 5 demonstrates the points which will be used for the polynomial fix, as well as the division of the panel into three subpanels.

3. Orthogonally project the polynomial fix points onto the $x_T - y_T$ plane. One can also project the edges of the panel onto the $x_T - y_T$ plane. The projection of the curved panel edges and polynomial fix points onto the $x_T - y_T$ plane forms a flat reference panel for the integration. This projection is demonstrated in figure 6 and figure 3.

4. Compute the integrand, $Q(r'_f, \theta'_f)$ at the polynomial fix points, which is product of the following values:

   (a) The determinant of the Jacobian of the mapping between the curved panel and the orthonormal projection of the panel onto the $x_T - y_T$ plane. The expression of the determinant can be found analytically for quadratic panels.

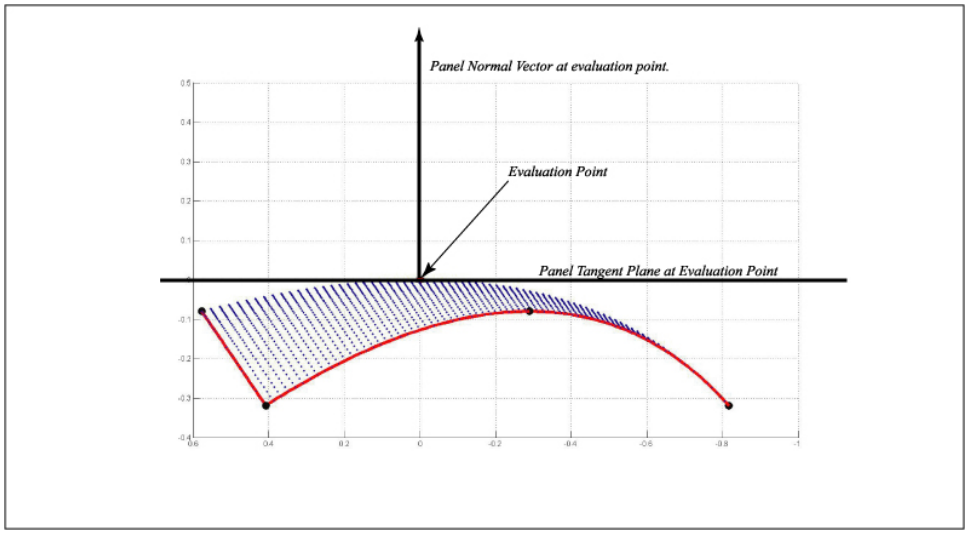

Figure 4. The panel after it has been appropriately transformed such that the tangent plane at the evaluation point is the $x_T - y_T$ plane, and the panel normal at the evaluation point is in the $+z_T$ direction.

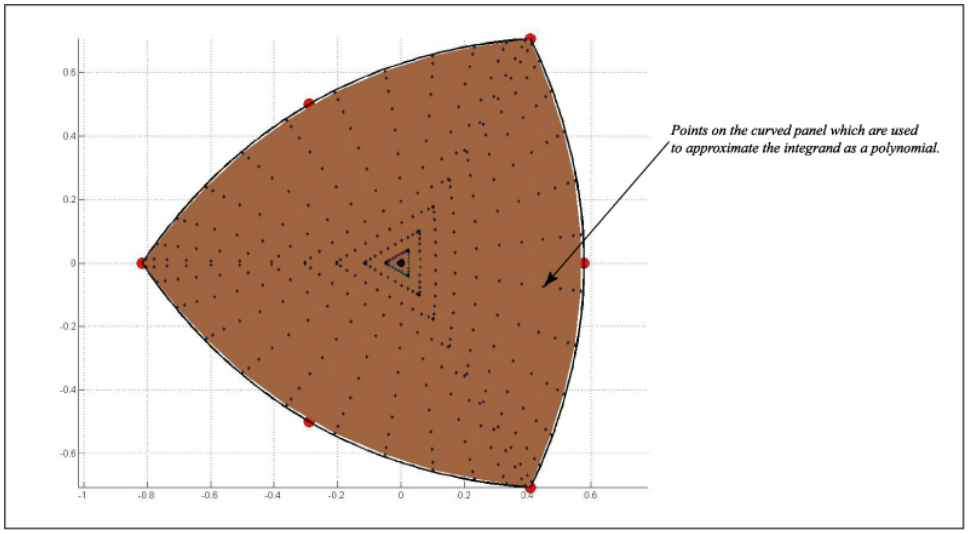

Figure 5. The points which are used to compute the polynomial approximation of the smooth integrand. Notice the polynomial fixing points are arranged in a manner that resembles a quadrature scheme for a degenerate quadrilateral. This apparent degeneracy will disappear once $R - \Theta$ coordinates are used. In addition, one should note the division of the panel into three subpanels. The layout of quadrature points and division of the panel is performed on the $s - t$ parametric triangle.

(b) The ratio between the kernel evaluated on the flat panel to the evaluation point and the kernel evaluated on the curved panel to the evaluation point.

(c) The Basis function value, $\sigma(r'_f, \theta'_f)$.

5. Compute a polynomial approximation to represent the integrand in the $R-\Theta$ coordinate system. This polynomial approximation is computed by a simple linear system solve (The right hand side vector

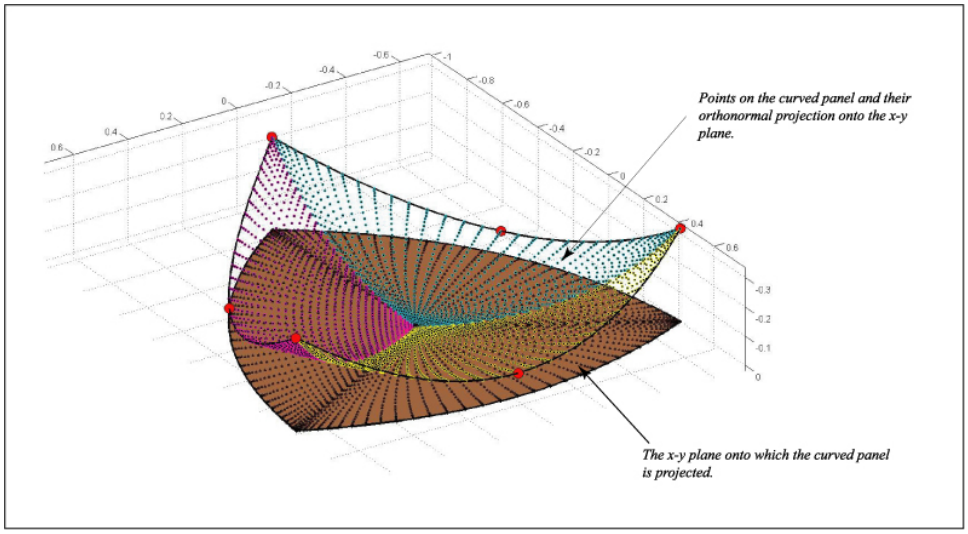

Figure 6. The orthonormal projection shown for a large selection of points on the curved panel. Note that the panel edges will not be straight lines in the general case. This is the fundamental difference between the Wang et al. method and the current method for computing the self term integration of the single layer.

contains the known values of the function, the system matrix is a Vandermonde matrix where the entries are evaluated at the polynomial fix points (in $R-\Theta$ coordinates), while the vector of unknowns contains the unknown polynomial coefficients.

6. Integrate the resulting polynomial in R analytically. The integrand of:

$$\Psi(x) = \int_{\Theta=0}^{\Theta=2\pi} \int_{r=0}^{r=R(\theta)} Q(r'_f, \theta'_f) dr d\theta' \tag{13}$$

is a polynomial representation in $R - \Theta$. As such, the integral is simply an appropriate coefficient multiplication and exponent augmentation. The integral becomes:

$$\Psi(x) = \int_{\Theta=0}^{\Theta=2\pi} U(R'_f(\theta'_f), \theta'_f) d\theta', \tag{14}$$

where $U(R'_f(\theta'_f), \theta'_f)$ is the polynomial resulting from integration. $R'_f(\theta)$ is the distance from the evaluation point to the flat panel edge for a given angle θ. This integral is merely an integration of $U(R'_f(\theta), \theta'_f)$ in θ around the edges of the panel.

7. Determine a quadratic parametric relation for the edges of the curved panel (a one-dimensional quadratic parametrization of the projected edge), such that in the parameter t the θ-integral becomes:

$$\Psi(x) = \int_{\Theta=0}^{\Theta=2\pi} U(R'_f(\theta), \theta'_f) d\theta' = \int_{t=0}^{t=1} U(R'_f(\theta'_f(t)), \theta'_f(t)) |J_{\theta \to t}| dt. \tag{15}$$

Since the above integral is computed numerically using quadrature, place quadrature points on the panel edges. These quadrature points are placed by mapping the Gauss quadrature points from the parametric representation to the curved edges.

8. Integrate the line integral numerically using the panel edge based quadrature routine.

The scheme presented for the single layer self term can be applied to arbitrary curved panels with high order basis functions. In addition, the method does not have the same limitations as the Wang et al. method due to the lack of restrictions on the reference panel edge shape. In the current method, the reference flat panel edges can be straight or curved lines. The curved panel self term single layer integration using the above process is simple from both an application and conceptual point of view.

B. Double Layer Integrals: Self Term

As with the single layer integration, the double layer self term integration approach we present is a conceptually simple numerical integration. Similar to the single layer, the approach we present for the double layer is not restricted simply to self term panels.

1. Background Theory

The double layer self term integral is performed through the implementation of some fundamental ideas presented in Kellogg[9] and later exploited in Newman.[7] The double layer expression is considered from a slightly different perspective as shown below:

$$\Phi(x) = \int_{S'} \mu(x') \frac{\partial}{\partial n} \frac{1}{\|x - x'\|} dS', \tag{16}$$

where $\mu(x')$ is the basis function representation. If we re-write the expression as:

$$\Phi(x) = \int_{S'} \mu(x') \hat{n} \cdot \left[\nabla \left(\frac{1}{\|x - x'\|} \right) \right] dS', \tag{17}$$

the the expression in the square brackets can be regarded as the velocity at the panel surface integration variable x' due to a point charge at x. Furthermore, if we assume that for now $\mu(x')$ is a constant over the panel:

$$\Phi(x) = \int_{S'} \hat{n} \cdot \left(\nabla \left(\frac{1}{\|x - x'\|} \right) \right) dS', \tag{18}$$

which is exactly the flux through the panel S' due to a point charge at x.

Since the point charge at x emits a divergence free velocity in a radial manner, we can equivalently say that the flux due to the point source which passes through the panel, is identical to the flux which passes through any radial projection of the panel (where the radial projection is centered at the point source which is also the evaluation point). If the panel is radially projected onto a unit sphere centered at the evaluation point, the integration is equivalent to determining the flux through a portion of a sphere defined by the radial projection of the panel. This is shown in figure 7.

The integral for the flux through the spherical patch formed by the radial projection of the panel is expressed as:

$$\Phi(x) = \int_{S'} \hat{n} \cdot \left(\nabla \left(\frac{1}{r} \right) \right) dS' = \int_{S'} \hat{n} \cdot \left(\nabla \left(\frac{1}{1} \right) \right) dS' \tag{19}$$

Which is identically the area of the sphere onto which the projection of the panel acts. In order to compute higher order distributions a similar radial projection can be used.In the higher order approach, the basis function is considered as a weighting function on the flux through the panel due to the source point charge. In other words, both the panel and the basis function are projected onto the unit sphere in a radial projection. This is shown by considering equation 17:

$$\Phi(x) = \int_{S'} \mu(x') \hat{n} \cdot \left[\nabla \left(\frac{1}{\|x - x'\|} \right) \right] dS'. \tag{20}$$

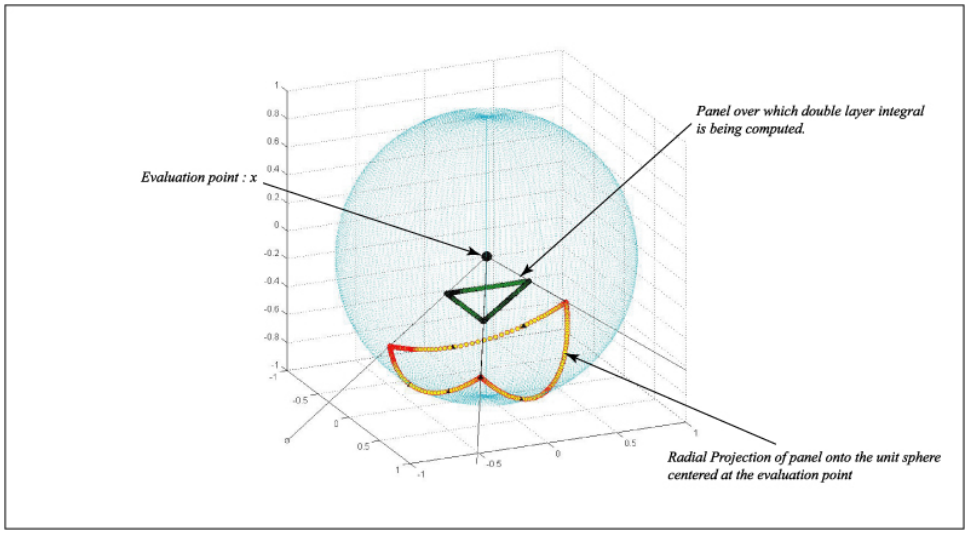

Figure 7. The radial projection of a flat panel onto the unit sphere centered at the evaluation point, x.

The interpretation of the dipole integral here is a flux through the panel surface S, due a point charge located at x, weighted with the basis function value $\mu(x')$ at the point x' at which the flux is being evaluated. Again, since the flux due to the source point charge is divergence free, this weighed flux for each point x' on the panel can be projected onto the unit sphere in a similar radial projection as before. The resulting integral becomes:

$$\Phi(x) = \int_{S'} \mu(\theta,\phi)\hat{n} \cdot \left(\nabla\left(\frac{1}{r}\right)\right) dS' = \int_{S'} \mu(\theta,\phi)\hat{n} \cdot \left(\nabla\left(\frac{1}{1}\right)\right) dS' \tag{21}$$

Which is merely a calculation of the basis function weighted area of the radially projected panel onto the unit sphere.

2. A Note on the Self Term Double Layer Potential Integral

When the self term of the double layer potential integral over a surface is considered, care must be taken. Consider the double layer integral:

$$\Phi(x) = \int_{S'} \mu(x') \frac{\partial}{\partial n} \frac{1}{\|x - x'\|} dS', \tag{22}$$

At $x = x'$, the integral is undefined. As such the point is excluded from the domain and the Cauchy Principle Value is evaluated, such that:

$$\Phi(x) = \pm 2\pi\mu(x) + \int_{S'} \mu(x') \frac{\partial}{\partial n} \frac{1}{\|x - x'\|} dS', \tag{23}$$

where the $\pm 2\pi$ term is the Cauchy Principle Value of the integral, the sign of which depends on the direction in which one approaches the panel (from above or below).The remaining integral is evaluated over all $x' \neq x$ points on the panel. In the section which follows, the evaluation of the integral is of interest and will be described.

3. Implementation Approach

The implementation of the integration of the double layer over curved panels is presented for quadratic basis functions; however, it should be noted that arbitrary order basis functions can be used. Furthermore, it

should be noted that the constant basis computation is much less rigorous than the higher order computations, since it amounts to computing the area of the sphere between the equator and the projection of the panel. This is a direct result of the fact that there is no basis distribution on the panel.

The following steps are performed to compute the double layer integral.

1. Transform the curved panel such that the tangent plane at the evaluation point lies in the $x_T - y_T$ plane, and the panel normal at the evaluation point is in the $+z_T$ direction, as shown in figure 4. Furthermore, translate the transformed panel such that the evaluation point lies at $(x_e, y_e, z_e) = (0, 0, 0)$.

2. Split the curved triangle into 6-sub triangles. These sub triangles are formed by:

   (a) Dividing the panel along lines joining the evaluation point and the vertices.

   (b) Dividing the panel along the lines joining the evaluation point and the nearest point on each of the panel edges (in the current implementation this is measured on the reference parameter based triangle).

3. Determine quadrature points on each of the six sub triangles. In addition to the points themselves, determine the basis function value at each of the points. These quadrature points are determined based on quadrature rules applied to the $s - t$ parameter triangles and then mapped to the surface of the curved panel. As in the single layer self term computation, these points are used for the determination of a polynomial approximant, hence they can be any appropriate distribution of points. Again, we choose to use the quadrature rule for four-sided domains. Figure 8 demonstrates the splitting of the curved triangle and the placement of quadrature points.

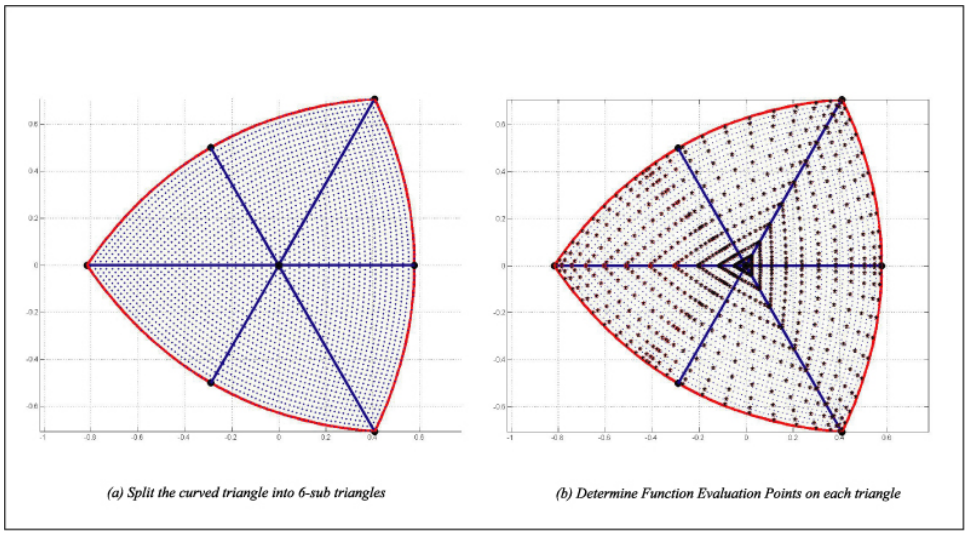

Figure 8. The 6-subtriangles illustrated on the curved panel. The illustration on the right shows the points which will be used in the polynomial approximation of the integrand after it is projected to the unit sphere.

4. Radially project the points on the panel onto the unit sphere. The points can be projected onto the unit sphere by:

$$P_S(x, y, z) = \frac{P(x, y, z)}{\|P(x, y, z)\|} \tag{24}$$

   Note, since the integral in question excludes the point $x = x'$, the projection of the portion of the panel directly encircling the origin (which is the evaluation point), will lie on the equator of the sphere.

By radially projecting the panel onto a unit sphere centered at the evaluation point, the integral can be represented as:

$$\Phi(x) = \oint_{S'} \mu(x') \frac{\partial}{\partial n} \frac{1}{\|x - x'\|} dS' \rightarrow \int_{\Theta=0}^{\Theta=2\pi} \int_{\Phi=0}^{\Phi=\phi(\Theta)} \mu(\phi, \theta) \frac{\partial}{\partial n} \left(\frac{1}{r}\right) r^2 \sin(\phi) d\phi d\theta \tag{25}$$

Which, when we consider the unit sphere ($r = 1$), becomes:

$$\Phi(x) = \int_{\theta=0}^{\theta=2\pi} \int_{\phi=\frac{\pi}{2}}^{\phi=\phi(\theta)} \mu(\phi, \theta) \sin(\phi) d\phi d\theta \tag{26}$$

If, the $\sin(\phi)$ term in the integrand is combined with the basis representation to give $P(\phi, \theta)$, the resulting integral expression is:

$$\Phi(x) = \int_{\Theta=0}^{\Theta=2\pi} \int_{\Phi=\frac{\pi}{2}}^{\Phi=\phi(\Theta)} P(\phi, \theta) d\phi d\theta \tag{27}$$

5. Determine the $\Phi - \Theta$ coordinates of each of the points.

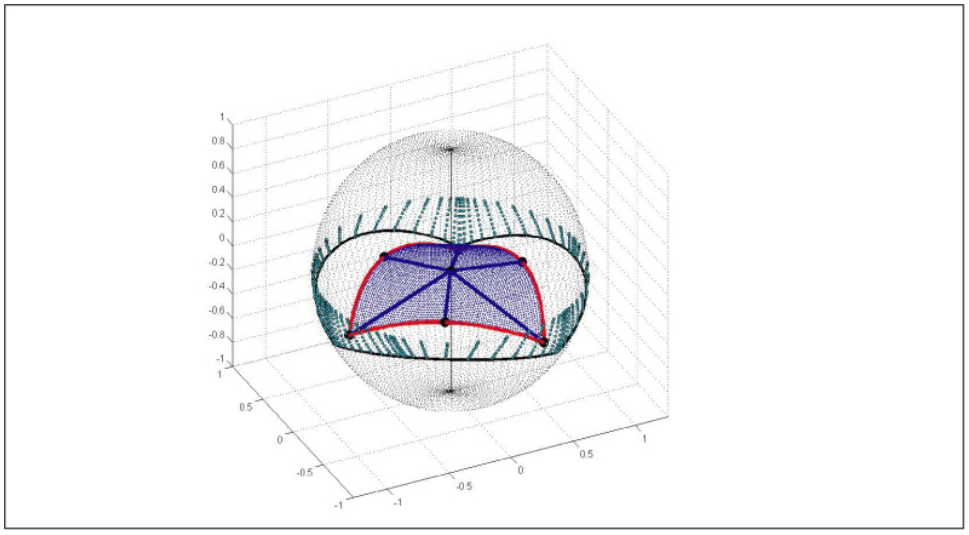

Figure 9. The radial projection of the points on the panel and the edges onto a unit sphere centered at the evaluation point.

6. Sort the projected points such that they lie within the Θ angles of the original curved panel subdivision.
7. For each of the 6 sub-triangles determine the polynomial approximation, $P(\phi, \theta)$, which best represents the basis function value as it is radially projected from the panel points to the points on the sphere.
8. Integrate the inner integral of the polynomial, $P(\phi, \theta)$, analytically in Φ:

$$\Phi(x) = \int_{\Theta=0}^{\Theta=2\pi} \int_{\Phi=\frac{\pi}{2}}^{\Phi=\phi(\Theta)} P(\phi, \theta) d\phi d\theta \rightarrow \Phi(x) = \int_{\Theta=0}^{\Theta=2\pi} Q(\phi(\Theta), \theta) d\theta \tag{28}$$

9. Integrate the remaining line integral using quadrature. The edge of the panel over which the line integral is being performed must be expressed as a quadratic line based on a parameter t. The integral to be computed then becomes:

$$\Phi(x) = \int_{t=0}^{t=1} Q(\phi(\Theta(t)), \theta(t))|J|_{\theta \to t} dt \tag{29}$$

Which is easily computed using moderate orders of Gaussian quadrature in one dimension.

10. Since we are concerned only with evaluating the Cauchy Principle Value integral in this computation, in order to get the full influence of the self term, we add to this result the appropriate $+/-2\pi$ Cauchy Principle Value (CPV).

VI. The Quadratic Basis, Quadratic Curvature Galerkin Panel Method

The high order panel method implemented in this paper is a Galerkin formulation[22] of the Green's Theorem BIE for potential flow. The evaluation of the integrals over the target panels in the Galerkin method is performed using Gauss Quadrature, while the inner panel integrals are computed using:

1. Gauss Quadrature for farfield interactions.
2. Wang et al.'s[6] method for nearby interactions.
3. Approaches described in sections V of this paper for the self term integrals.

A full linear system is constructed and a direct system solve is performed.

VII. Results

In order to demonstrate the new quadratic panel method, a series of solutions for the flow around increasingly refined unit spheres was examined. A plot of a 32-panel unit sphere geometry with both flat panels and planar panels is shown in figure 10. From the illustration, it is apparent that the quadratic panels are a large improvement to the geometry description over the traditional flat panel representation.

A. Potential Flow Around the Unit Sphere

The potential flow around the unit sphere has an analytical solution for the perturbation potential which is given by:[8]

$$\phi = U_\infty \cos\theta \left(\frac{R^3}{2r^2}\right). \tag{30}$$

The simulations considered were run at $U_\infty = 1$, over unit radius ($R = 1$) spheres. Using the analytical result as a reference, several different panel methods were compared. The panel method approximations which are considered are constant collocation on planar panels, linear basis Galerkin on planar panels, quadratic basis Galerkin on planar panels, and finally the new quadratic basis Galerkin approach on quadratic curved patches. The results of the quadratic curved panels are visibly superior to the constant collocation as presented in figure 11.

In order to examine the convergence rate as well as the accuracy of each of the panel methods studied, the convergence is demonstrated in figure 12. The error was computed for each panel and integrated using high order quadrature schemes.

From figure 12, it can be seen that the maximum permissible convergence rate for flat panel discretizations is limited by the geometry convergence. This is realized when comparing the quadratic, linear and constant basis solutions when flat panel discretizations are used. The flat panel discretization surface area

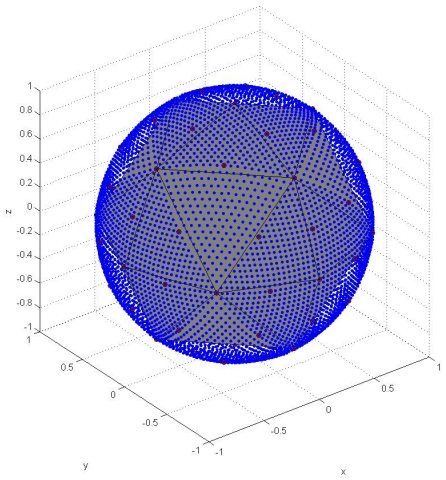

Figure 10. The unit sphere geometry demonstrating the flat panel and curved quadratic panel discretizations. The nodes of the quadratic panels are shown on the plot.

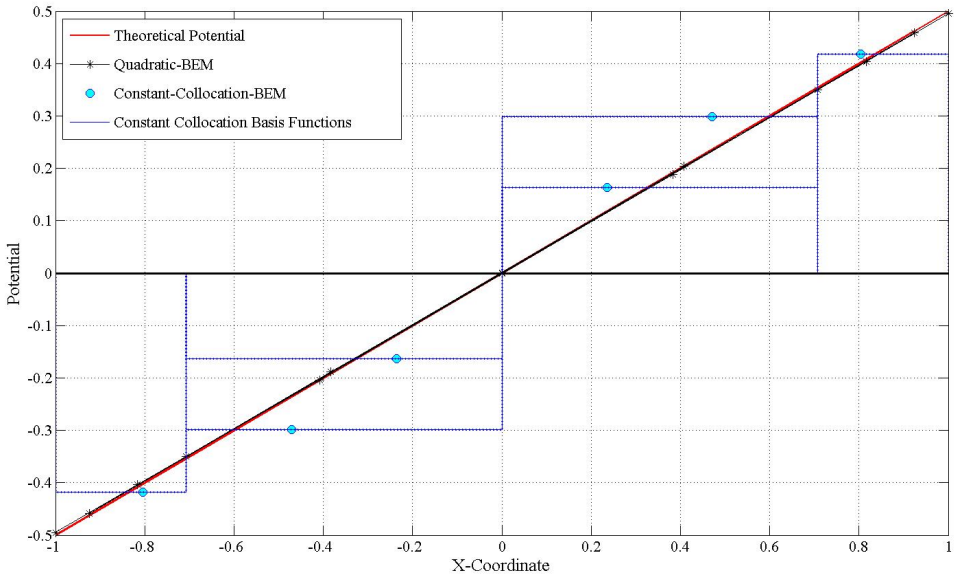

Figure 11. An illustration of the solution ϕ computed on a 32-panel sphere comparing constant basis function representations with quadratic basis functions on quadratic patches. The theoretical result is also plotted and coincides with the result from the high order panel method. For clarity in the depiction of the constant basis function results, both the potential value at the centroid and the basis function itself are represented on the plot. This further demonstrates that the constant basis approximation will have poor error convergence.

converges at a rate inversely proportional to the number of panels ($O(NP^{-1}) = O(h^2)$), hence becomes the limiting convergence rate for the case. It is interesting to note that the results for the linear basis function

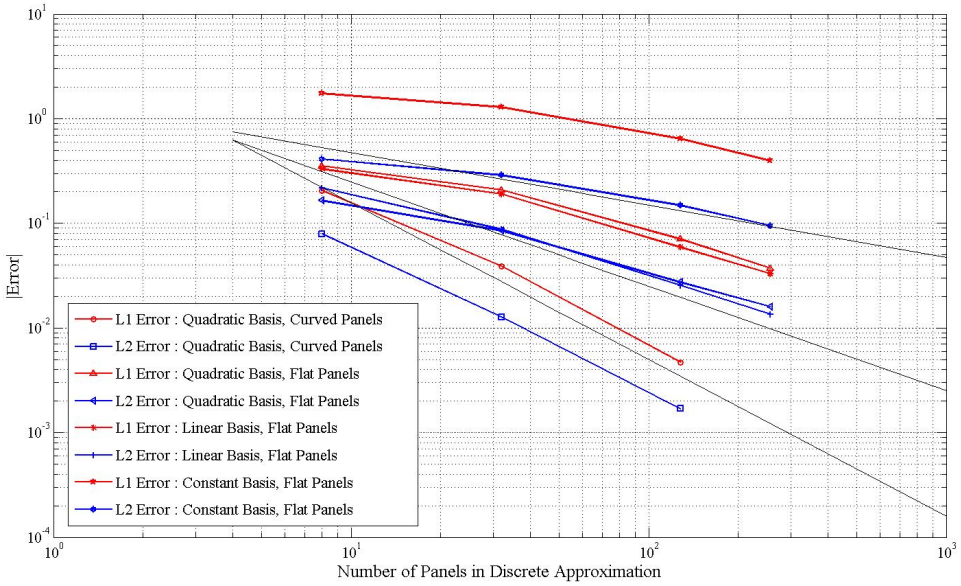

Figure 12. The error convergence of the potential for constant basis representation on flat panels, linear basis representation on flat panels, and quadratic representation on curved panels. The plots show L1 and L2 error integrated over the sphere using the underlying basis representation for the integration. Notice that the constant basis functions on flat panels converge at a rate of $O(NP^{-\frac{1}{2}})$, the linear basis on flat panels at $O(NP^{-1})$, the quadratic basis on flat panels at $O(NP^{-1})$, and the quadratic basis on quadratic patches at $O(NP^{-\frac{3}{2}})$.

representation are the most accurate of the set of computations done on flat panels. Although this may appear strange, it is consistent with the approximations being made. Quadratic basis functions will provide a more accurate solution to the discrete geometry (which is based on a flat panel representation), which in the case of a sphere or curved surface, is typically a worse approximation than the linear basis on flat panels.

The convergence results for the curved panel high order basis functions demonstrate that increased convergence rates can only be achieved if approximation order increases are realized in both basis function approximation and surface discretization. If we consider the panel methods described, it would take a discretization on the order of $10^5 - 10^6$ constant basis flat panels to achieve the error levels displayed by a 128 curved panel high order method. Similarly, it would take on the order of 10^4 panels to reach that level of accuracy using linear basis functions on flat panels. From these results it can be seen that low panel counts using accurate geometry representations and high order basis functions can often lead to accuracy levels hard to achieve with flat panel low order methods.

VIII. Conclusion

The work presented in this paper highlights the difficulties involved in computing panel integrals for the high order BEM representation and proposes approaches for integrating the self term integrals. It was found that the high order method, when compared on a number of panels basis was always significantly more accurate than the low order approaches.

IX. Future Work

With the integration techniques developed for quadratically curved panels with high order basis functions, the continued development of the high order panel method will include:

1. Incorporating the higher order integrals into an an iterative solution method coupled with a precorrected-FFT[4] acceleration technique.

2. With acceleration techniques in place, advanced wake models can be considered for lifting body simulations. Unsteady wake development and propagation through time stepping approaches such as those in FastAero[3] will be particularly benefited by higher order discretizations due to the shorter iteration times which are a direct result of the lower number of degrees of freedom for a given accuracy when using higher order methods.

Acknowledgments

The authors would like to express their gratitude to the Singapore-MIT Alliance, the National Sciences Foundation and the Natural Sciences and Engineering Research Council of Canada. The authors would like to also thank Mark Drela for providing valuable advice and discussions with regard to this research. In addition, we would like to thank Jaydeep Bardhan and Junghoon Lee for fruitful and lively discussions about panel integration and high order implementations. Finally, we would like to thank our wives and friends for their support.

References

[1]D. L. Ashby, M. R. Dudley, and S. K. Iguchi, *Development and Validation of an Advanced Low Order Panel Method*, NASA TM 101024, Oct 1988.

[2]B. Maskew,*PROGRAM VSAERO: A Computer Program for Calculating the Non-Linear Aerodynamic Characteristics of Arbitrary Configurations"*, NASA CR-166476, Nov 1982.

[3]D.J. Willis, J. Peraire, J.K. White, *A Combined pFFT-Multipole Tree Code, Unsteady Panel Method with Vortex Particle Wakes*, 43rd AIAA Aerospace sciences Meeting and Exhibit, AIAA-2005-0854, 10-13 January 2005.

[4]J. R. Philips and J. K. White, *A Precorrected-FFT Method for Electrostatic Analysis of Complicated 3-D Structures*, IEEE Transactions On Computer-Aided Design of Integrated Circuits and Systems, IEEE, Vol. 16, 1997.

[5]L. Greengard and V. Rohklin, *A Fast Algorithm for Particle Simulations*, J. Comp. Phys., 73:pp325-384, 1987.

[6]X. Wang, J.N.Newman, and J.K.White, *Robust Algorithms for Boundary Element Integrals on Curved Surfaces* , International Conference on Modeling and Simulation of Micro systems, 2000.

[7]J. N. Newman, *Distribution of Sources and Normal Dipoles Over a Quadrilateral Panel*, J. Eng. Math., 20, 1985.

[8]J. Katz, A. Plotkin, *Low-Speed Aerodynamics, 2nd Edition*, Cambridge university Press, New York, 2001.

[9]O.D.Kellogg *Foundations of Potential Theory*,J. Springer, New York, 1929.

[10]C.Y. Hsin, J.E.Kerwin, and J.N.Newman, *A high order panel method based on B-Splines*. Proceedings of Sixth International Conference on Numerical Ship Hydrodynamics, eds. V.C. Patel and F. Stern, National Academy Press: Washington, pp133-151, 1993.

[11]A.E. Magnus, and M.A.Epton, *PAN AIR- A Computer Program for predicting Subsonic or Supersonic Linear Potential Flows about Arbitrary Configurations Using a High Order Panel Method*, Volume 1, Theory Document (Version 1.0), NASA CR-3251, 1980.

[12]C.S. Lee and J.E. Kerwin, *A B-Spline Higher-Order Panel Method Applied to Two Dimensional Lifting Problems*, Journal Of Ship Research, Volume 47, Number 4, pp 290-298, 2003.

[13]P. Ramachandran, S.C. Rajan, M. Ramakrishna, *A Fast Multipole Method for Higher Order Vortex Panels in Two Dimensions*, SIAM Journal on Scientific Computing, Vol 26, Issue 5, pp. 1620-1642, 2005.

[14]H. Maniar, *A B-Spline Based Higher Order Method in 3D*, Presented at the 10th Workshop on Water Waves and Floating Bodies, Oxford, England, 1995.

[15]H. Maniar, *A Three Dimensional High Order Panel Method Based on B-splines*, PhD. Thesis, Massachusetts Institute Of Technology, 1995.

[16]F.E. Ehlers, F.T.Johnson, and P.E. Rubbert, *A Higher Order Panel Method for Linearized Supersonic Flow.* AIAA 76-381, July 1976.

[17]J. Hess, and A.M.O Smith, *Calculation of Non-lifting potential flow about arbitrary three dimensional bodies*, J. Ship Research, 8, pp 22-44, 1994.

[18]U. Lemma, V.Marchese,and L. Morino, *High-order BEM for potential transonic flows*, Computational Mechanics, Springer Verlag, Vol. 21, No. 3, pp. 243-252, 1998.

[19]J.H.M. Frijns, *Improving the Accuracy of the Boundary Element Method by the use of Second-Order Interpolation Functions.*, IEEE Transactions on Biomedical Engineering, Vol. 47, No. 10, October 2000.

[20]A. Buchau, W. Rieger, and W.M.Rucker *BEM Computations Using the Fast Multipole Method in Combination with Higher Order Elements and the Galerkin Method.*, IEEE Transactions on Magnetics, Vol. 37 No. 5, September 2001.

[21]K.J.Bathe *Finite Element Procedures*, Prentice Hall, 1995.

[22]K.E.Atkinson, and W.Han *Theoretical Numerical Analysis: A Functional Analysis Framework*, Springer-Verlag, 2001.